Fish and Shellfish Immunology 92 (2019) 772–781

Contents lists available at ScienceDirect

Fish and Shellfish Immunology

journal homepage: www.elsevier.com/locate/fsi

Full length article

A single-CRD C-type lectin (*Cg*CLec-3) with novel DIN motif exhibits versatile immune functions in *Crassostrea gigas*

Xiaorui Song[a,1], Xiaoyu Xin[a,1], Hao Wang[c], Hui Li[c], Huan Zhang[c], Zhihao Jia[c], Conghui Liu[c], Shuai Jiang[c], Lingling Wang[b,d], Linsheng Song[a,b,d,*]

[a] Liaoning Key Laboratory of Marine Animal Immunology, Dalian Ocean University, Dalian, 116023, China
[b] Laboratory of Marine Fisheries Science and Food Production Process, Qingdao National Laboratory for Marine Science and Technology, Qingdao, 266071, China
[c] Key Laboratory of Experimental Marine Biology, Institute of Oceanology, Chinese Academy of Sciences, Qingdao, 266071, China
[d] Liaoning Key Laboratory of Marine Animal Immunology & Disease Control, Dalian Ocean University, Dalian, 116023, China

ARTICLE INFO

Keywords:
Crassostrea gigas
C-type lectin
DIN motif
PAMP binding
Agglutination
Antibacterial activity

ABSTRACT

C-type lectins (CTLs), as important pattern recognition receptors (PRRs), are a superfamily of Ca^{2+}-dependent carbohydrate-recognition proteins which participate in nonself-recognition and eliminating pathogens. In the present study, a novel CTL (designated as *Cg*CLec-3) was identified from the Pacific oyster *Crassostrea gigas*. There was only one carbohydrate-recognition domain (CRD) of 151 amino acid residues within the deduced amino acid sequence of *Cg*CLec-3. The deduced amino acid sequence of *Cg*CLec-3 CRD shared low homology with the CRDs of other CTLs in oyster with the identities ranging from 12% to 22%. A novel DIN motif was found in Ca^{2+}-binding site 2 of *Cg*CLec-3. The relative expression level of *Cg*CLec-3 in hemocytes was up-regulated significantly after the stimulations of bacteria and Pathogen Associated Molecular Patterns (PAMPs). Immunohistochemistry assay showed that *Cg*CLec-3 protein was mainly distributed in gill and mantle, less in gonad, and could not be detected in adductor muscle and hepatopancreas. The recombinant protein (r*Cg*CLec-3) could bind lipopolysaccharide (LPS), mannose (MAN) and peptidoglycan (PGN), but not poly (I:C). r*Cg*CLec-3 exihibited strong binding ability to *Vibrio anguillarum* and *V. splendidus*, moderate binding activities to *Escherichia coli*, *Pichia pastoris* and *Yarrowia lipolytica*, weak binding affinity to *Staphylococcus aureus* and *Micrococcus luteus*. r*Cg*CLec-3 could agglutinate microorganisms, in a Ca^{2+}-dependent manner and its activity to agglutinate *V. splendidus* was remarkably higher than that to agglutinate *E. coli*, *S. aureus* and *P. pastoris*. The phagocytic activity of oyster hemocytes was significantly enhanced after incubation with r*Cg*CLec-3. r*Cg*CLec-3 also exhibited antibacterial activity against *E. coli* and *S. aureus*. The results clearly suggested that *Cg*CLec-3 in Pacific oyster *C. gigas* not only served as a PRR involved in the PAMPs recognition and microbes binding, but also functioned as an immune effector participating in the clearance of invaders.

1. Introduction

The invertebrates rely on their innate immunity to defend microbes as they lack of adaptive immune system [1,2]. The first and crucial step of innate immune response is to recognize a group of highly conserved molecules presented in most microorganisms (named as pathogen-associated molecular pattern, PAMPs) through a serial of pattern recognition receptors (PRRs) [3,4]. Among the known invertebrate PRRs, C-type lectins (CTLs) are a large and diverse group of carbohydrate-sensing proteins, which play vital roles in nonself recognition and elimination of invading microbes through recognizing and binding to terminal sugars on glycoproteins and glycolipids in a calcium (Ca^{2+})-dependent manner [5–7]. CTLs generally contain at least one carbohydrate recognition domain (CRD) consisted of ~130 amino acid residues with several conserved motifs, which endows CTLs with activities of recognition and clearance of invaders. There are four Ca^{2+}-binding sites in each CRD, among which the site 2 is known to be involved in the carbohydrate binding activity and specificity [6,8,9]. The invertebrate CTLs have been reported to play important roles in many immune processes such as PAMPs recognizing and binding, opsonization, and microbe elimination [10].

With rapid development of omics technique, large amounts of CTLs have been annotated and characterized in molluscs. For example, there is an expanded set of 266 CTLs annotated in the genome of oyster

* Corresponding author. Liaoning Key Laboratory of Marine Animal Immunology, Dalian Ocean University, Dalian, 116023, China.
E-mail address: lshsong@dlou.edu.cn (L. Song).
[1] These authors contributed equally.

https://doi.org/10.1016/j.fsi.2019.07.001
Received 5 April 2016; Received in revised form 1 July 2019; Accepted 1 July 2019
Available online 03 July 2019
1050-4648/

Crassostrea gigas [11]. Most of known molluscan CTLs have a single CRD, while some multi-CRD CTLs have also been identified from scallops and oysters recently [12–15]. Accumulating data have revealed that molluscan CTLs differ significantly in amino acid sequences of CRD [6,10]. The molluscan CRDs are much more diversified in the motif of the Ca^{2+}-binding sites 2 than that in vertebrates. Glu-Pro-Asn (EPN) and Gln-Pro-Asp (QPD) are generally considered as the conserved motifs in Ca^{2+}-binding site 2 of vertebrate CRDs, which have been demonstrated to bind mannose and galactose, respectively [6]. The conserved motifs EPN [16–18] and QPD [19] have also been identified in molluscan CRDs. Different from their specific binding characteristics in vertebrates, the EPN and QPD motif in molluscan CRD might be responsible for the recognition of broad-spectrum carbohydrates. For instance, *Cg*CLec-2 from *C. gigas* with EPN motif displayed a high affinity to lipopolysaccharide (LPS), peptidoglycan (PGN), and mannose (MAN) [16]. *Cf*Lec-3 from *Chlamys farreri* with EPN motif could bind LPS, PGN, and β-glucan (GLU) [18]. CRD4 from *Hyriopsis cumingii* with QPD motif could bind LPS and PGN [19]. Moreover, at least nine types of novel motifs have been so far reported in molluscs, including Glu-Pro-Asp (EPD) [20,21], Gln-Pro-Gly (QPG) [8], Gln-Pro-Ser (QPS) [22], Tyr-Pro-Gly (YPG) [10], Tyr-Pro-Thr (YPT) [12,14], Gln-Pro-Gly (QPE) [7], Gln-Tyr-Gly (QYE) [7], Gln-Pro-Asn (QPN) [14], and Tyr-Pro-Asp (YPD) [23]. Most of these novel motifs, such as QPE, QYE, EPD, YPT, QPN and YPD endow molluscan CTLs with binding capability to various carbohydrates [10,24,25]. Some molluscan CTLs with different motif at the Ca^{2+}-binding site 2 display similar PAMPs and microbial binding spectrums. For example, both *Cg*CLec-4 and *Cg*CLec-5 from *C. gigas* with QPE and QYE motif, respectively, could bind different PAMPs (LPS, PGN, GLU and MAN) and different kinds of microorganisms (*Staphylococcus aureus*, *Escherichia coli*, *Vibrio anguillarum* and *Yarrowia lipolytica*) [26]. Some molluscan CTLs with the same first motif of Ca^{2+}-binding site 2 displayed different PAMPs binding spectrums. In *C. farreri*, *Cf*Lec-1 containing EPD motif could bind LPS, PGN and MAN *in vitro* [27], while *Cf*Lec-2 with the same motif could also bind zymosan additionally [28]. Although the recognition mechanism and ligand affinity of molluscan CTLs are not well understood, the broad spectrums of recognition and binding endow them with important physiological functions during the immune response.

The increasing evidences have documented the involvement of CTLs in nonself recognition, agglutination, opsonization and phagocytosis in the innate immunity of molluscs. Some molluscan CTLs, such as *Cg*CLec-4, *Cg*CLec-5, *Ai*CTL-5 and *Ai*CTL-6, exhibited agglutinating activity towards various bacteria and fungi [7,14,20,21,29]. The purified MCL, MCL-3, and MCL-4 from the plasma of Manila clam *Ruditapes philippinarum* significantly enhanced the hemocyte phagocytic ability toward the bacteria, and also markedly suppressed the growth of *Alteromonas haloplanktis* [30,31]. Similarly, the recombinant CTLs *Cf*CLec-1 and *Cf*CLec-2 from *C. farreri* [27,28] and *Cg*CLec-2 and *Cg*CLec-4 from *C. gigas* [7,16] could inhibit the growth of several bacteria. Accumulating data have demonstrated that numerous molluscan CTLs exert efficient functions in the immune responses against invading pathogens.

The Pacific oyster *C. gigas* (Thunberg, 1793) is a marine bivalve belonging to the phylum Mollusca. The accumulating evidences indicate that oysters have evolved a highly complex innate immune system with remarkable discriminatory properties, which contributes indispensably to estuarine and intertidal regions [11,32]. The comprehensive genomic annotation revealed a great number of genes constituting the oyster immune system, among which the significant expansions were found in PRR families. Oysters exploit different PRRs with various domain structures to detect the signature molecules of pathogenic microbes [24]. There were 266 C-type lectin domain containing (CTLDs) proteins found in the Pacific oyster genome, which was much more than that in fruit fly (34 CTLDs) and human (81 CTLDs) [11,32]. Up to date, only four CTLs have been identified and functionally characterized from Pacific oyster *C. gigas* [7,16,33], while the knowledge about the domain organization, motif characterization and the detailed functions of most Pacific oyster CTLs are still very limited. In the present study, a novel CTL, *Cg*CLec-3 with a single CRD with six conserved cysteines and a novel DIN motif, was characterized from the Pacific oyster *C. gigas*. The tissue distribution of *Cg*CLec-3 protein, temporal expression pattern post bacterial challenge and PAMPs stimulation, as well as their functions in PAMPs and bacteria binding, agglutination, phagocytosis and microbe elimination, were investigated to enrich the basic knowledge of oyster CTLs.

2. Materials and methods

2.1. Oysters and immune challenge

The adult Pacific oyster *C. gigas*, with an average shell length of 13.0 cm, were obtained from a local farm in Qingdao, Shandong Province, China. The oysters were acclimated in the aerated seawater at ~20 °C for seven days before processing.

Pathogenic bacteria *V. splendidus* and *V. anguillarum* were cultured in 2216E media (5 g/L Tryptone, 1 g/L Yeast extract, 0.1 g/L Ferric phosphate, 1L filtered seawater) at 16 °C for 24 h and harvested by centrifuged at 3000 *g*, 4 °C for 10 min. The pellets were washed three times and re-suspended in filtered seawater at a final concentration of 2×10^8 CFU/mL.

Two hundred and sixteen oysters were employed in the bacterial challenge and PAMPs stimulation assay. They were randomly divided into six groups with 36 individuals in each group. The oysters in the experimental groups received an injection of 100 μL V. *splendidus* (2×10^8 CFU/mL), *V. anguillarum* (2×10^8 CFU/mL), LPS (1 mg/mL in PBS) from *E. coli* 0111:B4 (Sigma), PGN (0.8 mg/mL in PBS) from *S. aureus* (Sigma), and GLU (1.0 mg/mL in PBS) from baker's yeast *S. cerevisiae* (Sigma), respectively. The oysters in the control group received an injection of 100 μl filtered seawater. Six individuals were randomly collected from each group at 0, 3, 6, 9, 12 and 24 h after injection, respectively. The hemolymph was extracted from the hematococoel using a sterile syringe with pre-cooled modified Alsever's solution (MAS, glucose 20.8 g/L, sodium citrate 8.0 g/L, ethylenediamine tetraacetic acid 3.36 g/L, sodium chloride 22.5 g/L, pH 7.5) at the ratio of 1:1, and centrifuged at 800 *g*, 4 °C for 10 min to harvest the hemocytes for RNA extraction.

2.2. cDNA cloning and sequence analysis of CgCLec-3

Total mRNA was extracted from hemocytes using Trizol reagent (Invitrogen) according to the manufacture's protocol. The first-strand cDNA synthesis was carried out based on M-MLV RT Usage information using the DNase I (Promega) treated total mRNA as template and oligo (dT)-adaptor primer (Table 1). The reaction mixtures were incubated at 42 °C for 1 h, terminated by heating at 95 °C for 5 min. The cDNA mix was diluted to 1:100 and stored at 80 °C for subsequent quantitative Real-time PCR (qRT-PCR) analysis.

A pair of gene-specific primers *Cg*CLec-3-F and *Cg*CLec-3-R (Table 1) were designed according to the sequence information of *Cg*CLec-3 (accession number: LOC105324528) acquired on the website of NCBI (http://www.ncbi.nlm.nih.gov/). PCR product was cloned into pMD 19-T simple vector (Takara) and sequenced. The resulting cDNA sequence and deduced amino acid sequence of *Cg*CLec-3 were analyzed by using the Sequence Manipulation Suite (SMS) (http://www.bio-soft.net/sms/) and the Expert Protein Analysis System (http://www.expasy.org/). The domain architectures of *Cg*CLec-3 were revealed by the simple modular architecture research tool (SMART) version 4.0 (http://smart.embl-heidelberg.de/). The presumed tertiary structure of the CRD in *Cg*CLec-3 was established using the SWISS-MODEL prediction algorithm (http://swissmodel.expasy.org/) and displayed by RasMol_2.7.5 [34]. The Clustalw Multiple Alignment program (http://www.ebi.ac.uk/clustalw/) was used to create the multiple sequence

Table 1
Primers used in this paper.

Primer	Sequence (5′-3′)
Clone primers	
CgCLec-3-F	GCTGGTGGGAAAGCATTG
CgCLec-3-R	GGTAAATGACGGAATAAACG
RT primers	
RT-CgCLec-3-F	GGTTGCTGGTGGGAAAGCATTGTAT
RT-CgCLec-3-R	TGTCGGGAGAGGTCGTTGGTGAAG
RT-EF-F	AGTCACCAAGGCTGCACAGAAAG
RT-EF-R	TCCGACGTATTTCTTTGCGATGT
Recombination primers	
Re-CgCLec-3-F	CGGGTACC/GCTGGTGGGAAAGCATTG
Re-CgCLec-3-R	GGGGATCC/GCGTGTTCCTCTCGCAGATT
Sequencing primers	
M13-47	CGCCAGGGTTTTCCCAGTCACGAC
RV-M	GAGCGGATAACAATTTCACACAGG
T7 promoter	TGCTAGTTATTGCTCAGCGG
T7 terminator	TAATACGACTCACTATAGGG

alignment.

2.3. Quantitative real-time PCR analysis of CgCLec-3 mRNA expression

*Cg*CLec-3 mRNA expression was analyzed by SYBR Green fluorescent qRT-PCR on an ABI 7500 Real-time Thermal Cycler. One pair of gene specific primers RT-*Cg*CLec-3-F and RT-*Cg*CLec-3-R (Table 1) for *Cg*CLec-3 were used to amplify a fragment of 113 bp. Meanwhile, the oyster Elongation Factor (*Cg*EF) fragment amplified with primers RT-EF-F and RT-EF-R (Table 1) was used as internal control. The mRNA expression level of *Cg*CLec-3 was determined by $2^{-\Delta\Delta Ct}$ method [35]. All data were given in terms of relative mRNA expressed as mean ± S.E. (N = 6). The data were subjected to one-way analysis of variance (one-way ANOVA) followed by an unpaired, two-tailed *t*-test. Differences were considered significant at $p < 0.05$ and extremely significant at $p < 0.01$. The samples at 0 h were used as baseline expression in the experiment of investigating the expression patterns of *Cg*CLec-3 mRNA after challenge.

2.4. Recombinant expression and purification of recombinant CgCLec-3 protein

*Cg*CLec-3 proteins were recombinant expressed with pET-32a system (Novagen). The coding region of *Cg*CLec-3 was amplified by the primers Re-*Cg*CLec-3-F and Re-*Cg*CLec-3-R with, *BamH* I and *Kpn* I endonuclease digestion sites at their 5' end, respectively (Table 1) from the pMD 19-T simple vector carrying full open reading frame of *Cg*CLec-3 (642 bp). The PCR products were digested with *BamH* I and *Kpn* I endonucleases, gel-purified, ligated to pET-32a plasmid which was obtained in the same way, and verified by DNA sequencing to construct the expression vector pET-32a-*Cg*CLec-3. The constructed expression plasmid was transformed into *E. coli* BL21 (DE3) (TransGen Biotech). The positive colony was incubated in LB medium (containing 50 μg/mL of ampicillin) at 37 °C with shaking at 220 rpm. The cells were incubated for another 4 h till the OD600 of the culture mediums reached to 0.4–0.6, and then isopropyl-β-d-thiogalactoside (IPTG) was added to the LB medium at the final concentration of 1 mM. The recombinant protein *Cg*CLec-3 (designated r*Cg*CLec-3) was purified by a Ni^{2+} chelating Sepharose column (Beijing Wei shi bo hui chromatographic technology co. LTD), eluted by 400 mM imidazole under denatured condition (8 M urea). The purified proteins were re-natured in gradient urea-TBS glycerol buffer (50 mM Tris-HCl, 50 mM NaCl, 15% glycerol, 2 mM reduced glutathione, 0.2 mM oxide glutathione, a gradient urea concentration of 6, 4, 3, 2, 1, 0 mM, pH 7.6; each gradient at 4 °C for 12 h). Protein concentration was determined by BCA method [36].

2.5. Polyclonal antibody preparation and western blot analysis

In order to prepare polyclonal antibody, the re-natured r*Cg*CLec-3 was dialyzed continuously against ddH_2O before the protein was freeze concentrated. The purified r*Cg*CLec-3 was immuned to 6-weeks old rats to acquire polyclonal antibody according to the previously described method [37]. Briefly, three 6-weeks female rats were acclimated in lab for seven days prior to use. On the 1st day, three 6-weeks female rats were inoculated intraperitoneally with 100 μg of r*Cg*CLec-3 (1 mg/mL) with an equal part of complete Freund's adjuvant (Sigma). On the 15th day, booster immunizations were given to each rat intraperitoneally with 100 μg of r*Cg*CLec-3 (1 mg/mL) in incomplete Freund's adjuvant (Sigma). Other two booster injections were given by tail vein with 50 μg of r*Cg*CLec-3 on the 22nd and 30th day. Seven days after the last injection, the blood was drawn from the posterior venous plexus of rat and obliquely placed at 4 °C overnight. The immune serum was collected after centrifugation at 4 °C, 3000 *g* for 30 min, and the specificity of *anti-Cg*CLec-3 antibody was identified by Western blot.

Briefly, proteins were transferred onto a 0.45 μm pore nitrocellulose membrane. After SDS-PAGE (12% gel), the membrane was blocked in TBST (50 mM Tris-HCl, 150 mM NaCl, 1‰ Tween 20) containing 5% skim milk powder at 37 °C for 1 h, then incubated with rat *anti*-r*Cg*CLec-3 antibody (1:800) for 1 h at 37 °C and washed three times with TBST. HRP-labeled anti-rat IgG (1:2000) was further incubated as the second antibody at 37 °C for 1 h, and the membrane was washed three times with TBST. After incubated in Western lighting-ECL substrate system (Thermo Scientific), the membrane was exposed to AI600 RGB (GE).

2.6. Immunohistochemistry of rCgCLec-3 in tissues

Immunohistochemistry (IHC) was used to detect the tissue distribution of *Cg*CLec-3 according to the method described by Jemaa et al. [38] with some modification. Tissues including gonad, gill, mantle, adductor muscle and hepatopancreas were fixed by using Bouin's fixative (Saturated picric acid solution: formaldehyde: glacial acetic acid = 15:5:1) at room temperature for 24 h. Then tissue samples were washed in 70% ethanol for 4 times (2 h each) and dehydrated in 80%, 95% and 100% successive ethanol baths for 1 h each, and then soaked in Xylene-ethanol solution (ration 1:1) for 1 h. Tissue samples were placed in Xylene for 1 h twice and then embedding the in paraffin. Cross-sections (5 μm) were cut by using an RM-2016 microtome (LEIKA). Paraffin was eliminated in Xylene bath and sections were rehydrated in successive 95%, 80%, 70%, 50% and 30% ethanol baths and then washed with distilled water. Sections were incubated with *anti*-r*Cg*CLec-3 antibody (1:500) at 37 °C for 1 h. After thoroughly washed with PBST, the sections were incubated with Alexa Fluer 488-labeled goat-*anti*-rat antibody (diluted 1:1000 in 3% BSA in PBST with Evans blue dye) for 50 min at 37 °C. Negative serum was performed as negative control. After three PBST washes, the sections were observed by using BX51 fluorescence microscopy (Olympus).

2.7. PAMPs binding assay

The dose-dependent PAMPs binding activity of r*Cg*CLec-3 was measured according to the previously reported methods [31] with minor modification. Briefly, 10 μg of LPS (Sigma), MAN (Sigma), PGN (Sigma) and poly (I:C) (GE Health) were used to coat a 96-well microtiter plate in 100 μl of carbonate-bicarbonate buffer (50 mM, pH9.6). In order to prevent the nonspecific adsorption, the wells were blocked with 200 μl of 3% BSA in TBST at 37 °C for 1 h. Then 100 μl of r*Cg*CLec-3 of several concentrations was added to the wells with 10 mM $CaCl_2$ and incubated for 3 h at 18 °C. The wells filled with 100 μl of TBS and rTrx were used as blank and negative control, respectively. Then 100 μl rats' immune serum of r*Cg*CLec-3 (1:1000 in 3% BSA) was used as the primary antibody and incubation at 37 °C for 1 h. The wells were washed three times with TBST between each incubation step. After that,

100 μl of HRP (horseradish peroxidase)-labeled anti-rat IgG (1:3000 in 3% BSA, Abcam) was further incubated as the second antibody. After three times with TBST, 100 μl of soluble TMB substrate solution was added and incubated at room temperature in dark for 30 min. The reaction was stopped by H_2SO_4 (2 moL/L) and the absorbance was read at 405 nm. The assay results were given in terms of the mean of three individual measurements ± S.E. (N = 3). Samples with P (sample)-B (blank)/N (negative)-B (blank) > 2.1 were considered as positive. There were three repeats in each group.

2.8. Microbial-binding assay

Microbial-binding activity was measured according to previous report with minor modification [17]. Gram-negative bacteria (*V. splendidus*, *V. anguillarum* and *E. coli*), Gram-positive bacteria (*S. aureus* and *Micrococcus luteus*) and fungi (*Pichia pastoris* and *Y. lipolytica*) were used to detect the microbial-binding activity of r*Cg*CLec-3. The microbes were suspended in TBS (OD600 = 2) and incubated with r*Cg*CLec-3 (20 μl, 0.25 mg/mL) in the presence or absence of 10 mM $CaCl_2$ at 4 °C overnight. After three times washes with TBS, the bound proteins were dissociated from the microorganisms by loading buffer and analyzed by SDS-PAGE and Western blot.

2.9. Microbial agglutination assay

The microbial agglutination assay was performed according to the description of previous report [18] with minor modification. The FITC-labeled Gram-negative bacteria (*E. coli* and *V. splendidus*), Gram-positive bacteria (*S. aureus*) and fungi (*P. pastoris*) were suspended in TBS buffer at 1×10^8 cells/mL. Then 10 μl of FITC-labeled microbes were incubated with r*Cg*CLec-3 (25 μl, 0.5 mg/mL) in the presence or absence of 10 mM $CaCl_2$. TBS and rTrx were performed as blank and negative control, respectively. After rotation in dark for 1 h, bacteria were observed under fluorescence microscopy (Zeiss).

2.10. Phagocytosis assay by FACScan flow cytometry

Phagocytosis assay was performed according to previous method with modification [27]. Briefly, 20 μl of FITC labeled *V. splendidus* (1×10^8 cells/mL) and 100 μl of r*Cg*CLec-3 (1 mg/mL) were mixed and rotated in dark at room temperature for 1 h. The hemolymph was extracted from the hematococoel of six oysters using a sterile syringe with pre-cooled modified Alsever's solution at the ratio of 1:1, and then centrifuged at 800 *g* for 10 min. The hemocytes were re-suspended in modified L-15 medium (M-L15, supplemented with 0.54 g/L KCl, 0.6 g/L $CaCl_2$, 1 g/L $MgSO_4$, 3.9 g/L $MgCl_2$, 20.2 g/L NaCl) at a final concentration of 1×10^6/mL. Then 200 μl of hemocytes suspension was added into the mixture and incubated for another 1 h. The mixture was centrifuged at 800 *g* for 10 min and re-suspended in 400 μL M-L15. The opsonization of r*Cg*CLec-3 was evaluated by FACScan flow cytometry (BD Biosciences). TBS and rTrx were used as blank and negative control, respectively. There were three repeats for each group.

2.11. The assay of antibacterial activity of rCgCLec-3

The growth curves of *E. coli* and *S. aureus* cultured with r*Cg*CLec-3 were tested as previous report with some modification [20]. *E. coli* or *S. aureus* in logarithmic phase were centrifuged, washed by TBS, and then re-suspended in TBS (1×10^4 CFU/mL). Fifty microliters of r*Cg*CLec-3 (2 mg/mL or 4 mg/mL) and the same volume of *E. coli* and *S. aureus* were mixed with $CaCl_2$ (the final concentration was 10 mM) and incubated at room temperature for 2 h. TBS and rTrx were performed as blank and negative control, respectively. Twenty microliters of the mixture was added into a 96-well microliter plate with 200 μl of LB medium. *E. coli* and *S. aureus* were cultured in 96-well microliter plates which were placed in microplate reader (Biotek) at 37 °C with shaking, respectively. OD_{600} was measured every 1 h from 13 h to 16 h to detect the growth of *E. coli* and *S. aureus*. Each group was repeated for three times.

2.12. Statistical analysis

All data were graphed and analyzed using Origin 8.1 (OriginLab) and Statistical Package for Social Sciences (SPSS) 16.0. Significant differences between treatments for each assay were tested by one-way analysis of variance (ANOVA). If significant differences were indicated at the 0.05 level, then a post hoc multiple-comparisons (Tukey's) test was used to examine significant differences among treatments using SPSS. Difference was considered significant at $p < 0.05$ and extremely significant at $p < 0.01$.

3. Results

3.1. cDNA cloning and sequence analysis of CgCLec-3

The complete open reading frame of *Cg*CLec-3 (642 bp) was obtained by PCR amplification. It encoded a polypeptide of 214 amino acids with a predicted molecular mass of about 21.36 kDa and a theoretical isoelectric point of 6.3. All the signature sequences of the CTL superfamily were identified in *Cg*CLec-3 by multiple sequences alignment of CRDs in *Cg*CLec-3 with those of other CTLs in Pacific oyster *C. gigas*. There is a signal peptide (1-19) and only one CRD consisting of 151 amino acid residues in *Cg*CLec-3. The CRD domain of *Cg*CLec-3 shared low sequence similarity with that of the previous reported CTLs from *C. gigas*, i.e. 18.79%, 21.22%, 15.76% and 12.12% identities with *Cg*CLec-1, *Cg*CLec-2, *Cg*CLec-4 and *Cg*CLec-5, respectively. A potential novel motif DIN (Asp148-Ile149-Asn150) was identified in Ca^{2+}-binding site 2. There were two potential disulfide bridges formed by Cys 60-Cys 181, and Cys 157-Cys 173, respectively. In addition, another two cysteine residues were located at the N-terminus (positions Cys 32 and Cys 43) of the CRD, indicating that the CRD was of long-form (Fig. 1 and Fig. 2).

The potential tertiary structure of CRD in *Cg*CLec-3 was established by SWISS-MODEL prediction algorithm based on the template 1TDQ.B. The DIN motif (Fig. S1, red dot) was located at the potential Ca^{2+}-binding site 2 and coincided with QPD motif in 1TDQ.B (Fig. S1, yellow dot), indicating that DIN motif might involve in carbohydrate binding and recognition of *Cg*CLec-3.

3.2. The expression patterns of CgCLec-3 mRNA after bacterial challenge and PAMPs stimulation

The mRNA expression patterns of *Cg*CLec-3 in hemocytes were analyzed by qRT-PCR after the bacterial (*V. splendidus* and *V. anguillarum*) challenge and PAMP (LPS, PGN and GLU) stimulations. *Cg*CLec-3 mRNA transcripts were significantly up-regulated compared to the seawater treatment group at 6 h and 9 h after both bacterial challenge and PAMP stimulations.

In the bacterial challenge experiments, the mRNA expression of *Cg*CLec-3 in hemocytes was up-regulated significantly at 6 h (6.65-fold compared to the control group, $p < 0.05$) post *V. splendidus* challenge and reached the maximum level at 9 h (15.73-fold, $p < 0.01$). Then it was down-regulated to 3.56-fold at 12 h ($p < 0.05$) and gradually recovered to the original expression level at 24 h (Fig. 3A). In the *V. anguillarum* challenge assay, the up-regulation of *Cg*CLec-3 mRNA transcripts occurred at 6 h post challenge (6.86-fold, $p < 0.05$), and the mRNA expression level decreased gradually to 4.02-fold at 9 h ($p < 0.05$) and 2.72-fold at 12 h ($p < 0.05$), respectively (Fig. 3B). No significant change of *Cg*CLec-3 mRNA expression was observed in the seawater group.

After LPS stimulation, the *Cg*CLec-3 mRNA expression was up-regulated from 3 h (19.95-fold, $p < 0.01$), dramatically reached the

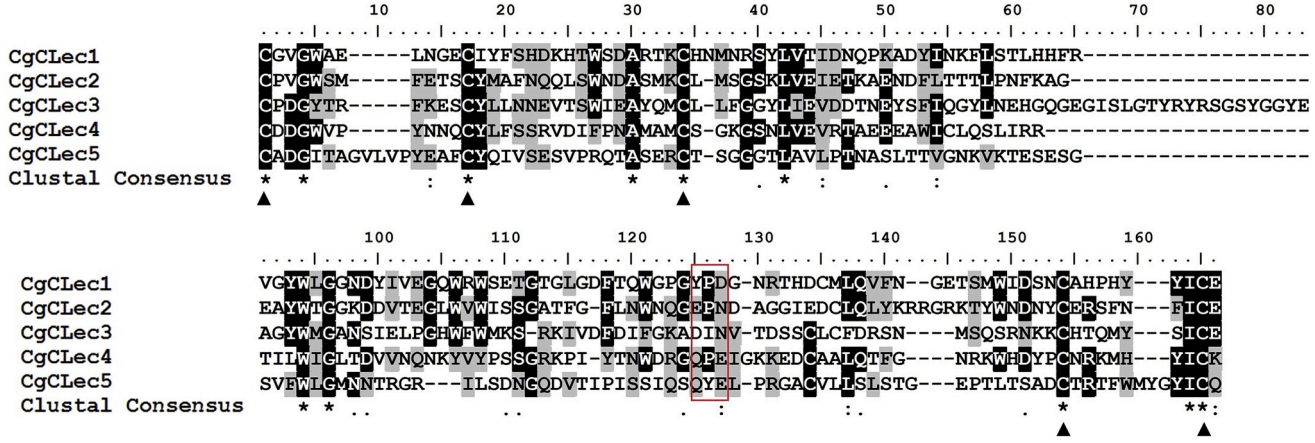

Fig. 1. Multiple sequence alignment by ClustalW of CRDs in *Cg*CLec-3 with other identified CRDs of CTLs in oyster. Proteins analyzed are list below: *Cg*CLec-1 (Accession No. BAF75353.1), *Cg*CLec-2 (Accession No. JH818449), *Cg*CLec-4 (Accession No. XP_011415552.1), and *Cg*CLec-5 (Accession No. EKC39564). The black shadow region means all sequences share the same amino acid residue, and the grey shadow indicates the amino acids with similarity more than 50%. Gaps are indicated by dashes to improve the alignment. "*" indicates positions which have a single, fully conserved residue. ":" indicates that one of the following 'strong' groups is fully conserved. "." indicates that one of the following 'weaker' groups is fully conserved. Conserved cysteine residues involved in the formation of the CRD internal disulfide bridges were marked as "*". The letters in box indicate the motif for determining ligand binding specificity.

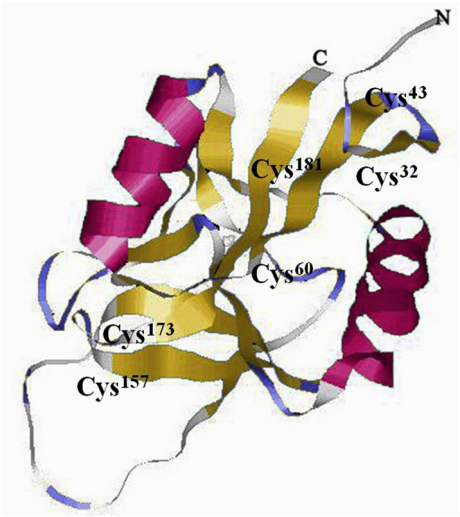

Fig. 2. The spatial structure of CRD in *Cg*CLec-3 predicted by SWISS-MODEL program. Random coil marked as white, β-stands marked as yellow and α-helices marked as red. There are four cysteines (Cys 60, Cys 157, Cys 173, and Cys 181) involved in forming disulfide bridges at the bases of the loops. (For interpretation of the references to color in this figure legend, the reader is referred to the Web version of this article.)

peak level at 9 h post stimulation (1390.24-fold, $p < 0.01$), and rapidly recovered to the original expression level at 12 h (Fig. 3C). In PGN and GLU treatment groups, the expression of *Cg*CLec-3 mRNA peaked at 6 h, which was earlier than that in LPS stimulation assay. However, the peak expression levels of *Cg*CLec-3 mRNA in PGN (6.32-fold, $p < 0.05$) (Fig. 3D) and GLU (14.05- fold, $p < 0.01$) (Fig. 3E) stimulation groups were lower than that in LPS stimulation group. There was no significant change of *Cg*CLec-3 mRNA expression in the seawater group during the experiment.

3.3. The prokaryotic expression of CgCLec-3 and western blot analysis

The purified r*Cg*CLec-3 was analyzed by SDS-PAGE. One distinct band with molecular weight of ~44 kDa was revealed, which was consistent with the predicted molecular weight of r*Cg*CLec-3 (Fig. 4A, lane 2–3). The purified r*Cg*CLec-3 (Fig. 4A, lane 4) was used to prepare antibody. The specificity of *Cg*CLec-3 antibody was detected by Western blot and a clear band of *Cg*CLec-3 with high specificity was identified (Fig. 4B, lane 1). One distinct band with molecular mass of ~22 kDa was revealed for rTrx, which was consistent with the predicted (Fig. 4C, lane 3). As a negative control, no notable band was detected in group of rat pre-immune serum (data not shown).

3.4. The distribution of CgCLec-3 in different tissues

The tissue distribution of *Cg*CLec-3 protein was investigated by immunohistochemistry in different tissues including gonad, mantle, gill, adductor muscle, and hepatopancreas. The positive signals of *Cg*CLec-3 were detected in gonad, mantle and gill tissues (Fig. 5 A1, B1 and C1), while no obvious positive signals were found in the adductor muscle and hepatopancreas tissues (Fig. 5 D1 and E1). In the gonad, the *Cg*CLec-3 protein was scatteredly distributed through the whole tissue. Strong positive signals of *Cg*CLec-3 could be detected on the epidermis cells of mantle edge. In the gill, *Cg*CLec-3 could be detected around the water tube. There was no obviously positive signal detected in adductor muscle, hepatopancreas, or control groups (Fig. 5).

3.5. PAMP-binding specificity of rCgCLec-3

The PAMP-binding capacity was recorded as P/N at 405 nm, and the samples with P/N > 2.1 were considered as positive. In the presence of Ca^{2+}, the P/N values for LPS, MAN, GLU, LTA and poly (I:C) were higher than 2.1, with the concentration of 100 μg/mL, 80 μg/mL, 60 μg/mL, 40 μg/mL, 20 μg/mL, respectively. r*Cg*CLec-3 exhibited the highest affinity to PGN, higher affinity to MAN and LPS, while almost no affinity to poly (I:C). The values of P/N were increased corresponding with the increase of r*Cg*CLec-3 concentration, which suggested that the binding activities of r*Cg*CLec-3 towards LPS, MAN and PGN were dose-dependent. As a control, the TBS was not able to bind any PAMPs (Fig. 6).

3.6. Binding of rCgCLec-3 to microbes

Western blot was used to investigate the binding activity of r*Cg*CLec-3 to microbes (Fig. 7). r*Cg*CLec-3 could bind to all the tested Gram-negative bacteria, Gram-positive bacteria, and fungi. In detail, r*Cg*CLec-3 displayed a strong binding capability to gram-negative bacteria *V. anguillarum* and *V. splendidus*. It could also bind to Gram-negative bacteria *E. coli*, fungi *Y. lipolytica* and *P. pastoris*, but showed very weak bind affinity to Gram-positive bacteria *S. aureus* and *M. luteus*. As

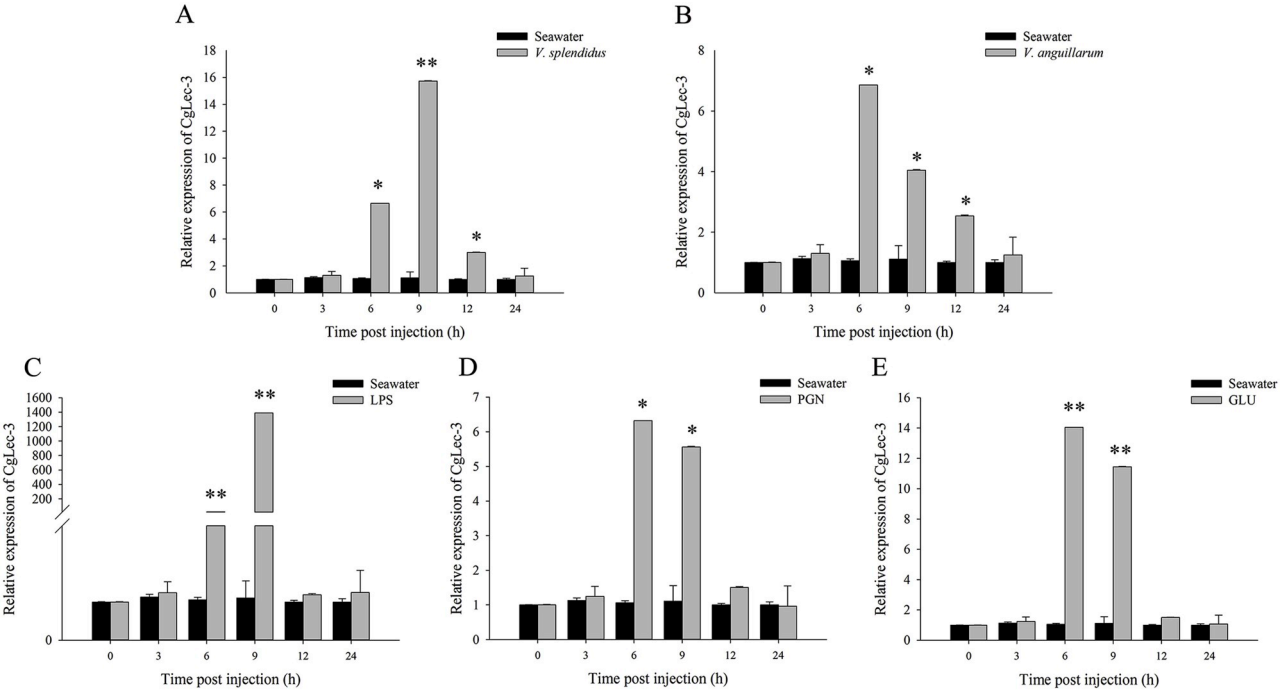

Fig. 3. The mRNA transcription patterns of *Cg*CLec-3 post bacterial and PAMP stimulations. *Cg*EF gene was used as an internal control to calibrate the cDNA template for all the samples. Each value was shown as mean ± S.D. (N = 3). The significant differences among the control and treated groups were subjected to one-way analysis of variance (one-way ANOVA). (**: $p < 0.01$; *: $p < 0.05$).

a control, no binding affinity was found in the group of rTrx (Fig. 7).

3.7. Microbial agglutinating activity of rCgCLec-3

Microorganisms *E. coli*, *V. splendidus*, *S. aureus* and *P. pastoris* were used to test the agglutinating activity of r*Cg*CLec-3. In the group of TBS with no Ca^{2+} group, there was no agglutination of the microbes in the visual field (Fig. 8, lane A). Similarly, no agglutination of the microbes was observed in the groups treated by r*Cg*CLec-3 without Ca^{2+} (Fig. 8, lane B). In the presence of Ca^{2+}, r*Cg*CLec-3 showed strong agglutinating activity to *V. splendidus*, but no agglutination was observed in *E. coli*, *S. aureus,* and *P. pastoris* groups (Fig. 8, lane C).

3.8. Phagocytic activity of oyster hemocytes enhanced by rCgCLec-3

The phagocytic activity of oyster hemocytes was quantified by flow cytometry analysis. After the hemocytes were co-incubated with r*Cg*CLec-3 and *V. splendidus* for 1 h, their phagocytic rate towards *V. splendidus* was 20.4%, which was significantly higher than those treated by TBS and rTrx (7.2% and 5.6%, $p < 0.05$), respectively. These results showed that the phagocytic activity of oyster hemocytes was significantly enhanced by r*Cg*CLec-3 (Fig. 9).

3.9. Antibacterial activity of rCgCLec-3

The antibacterial activity of r*Cg*CLec-3 was evaluated by detecting the bacteria growth curve. Gram-negative bacteria *E. coli* and Gram-positive bacteria *S. aureus* were cultured with LB medium. The OD_{600}

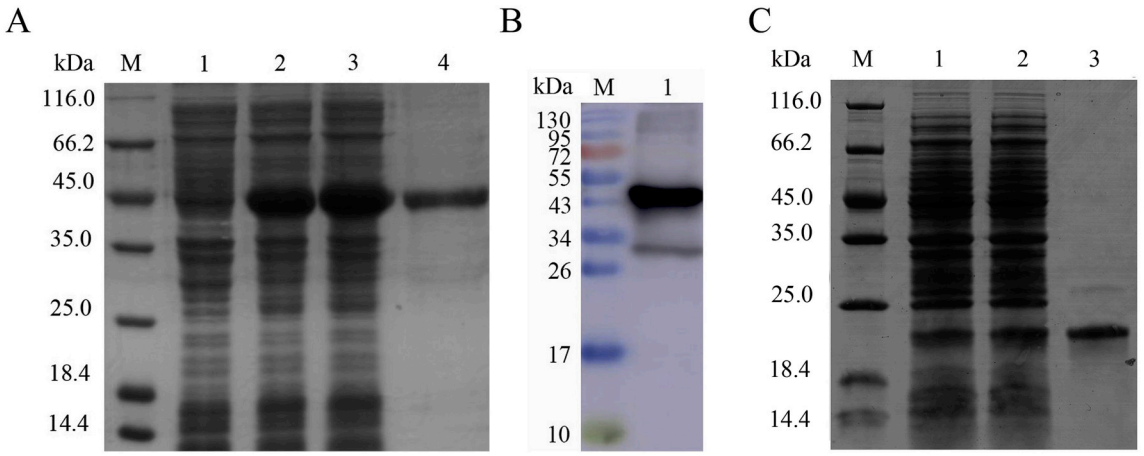

Fig. 4. SDS–PAGE and western-blot analysis of r*Cg*CLec-3. A: SDS-PAGE of rCgCLec-3. lane M: protein molecular standard (kDa); lane 1: negative control for r*Cg*CLec-3 (without induction); lane 2 and lane 3: induced r*Cg*CLec-3 with rTrx; lane 4: purified protein. B: western-blot analysis of *anti*-r*Cg*CLec-3. lane 1: Western blot based on the sample of lane 4. C: SDS-PAGE of rTrx. lane 1: negative control for rTrx (without induction); lane 2: induced rTrx; lane 3: purified rTrx.

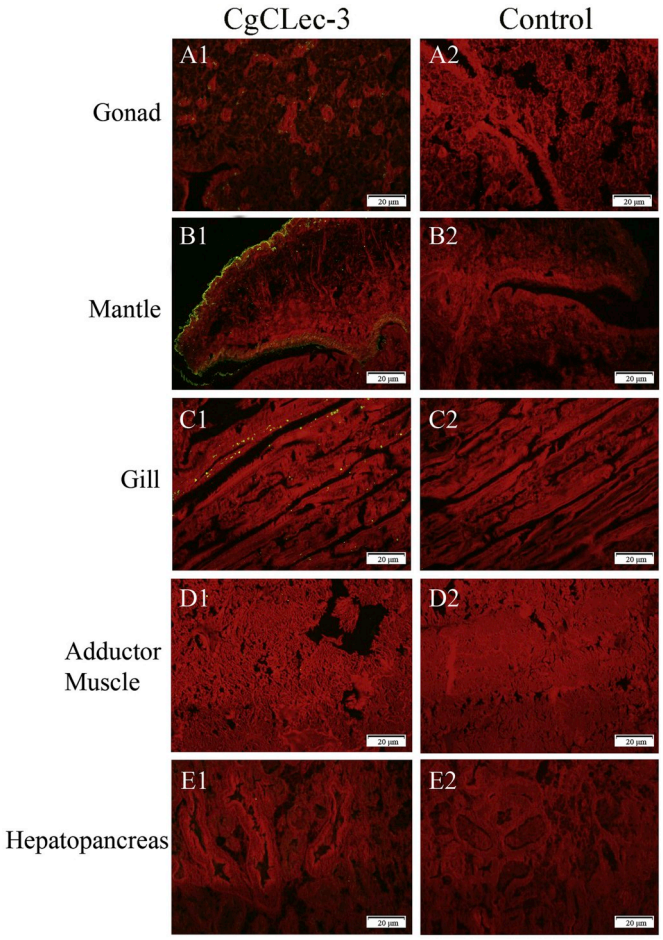

Fig. 5. The expression of *Cg*CLec-3 protein in different tissues of oyster *C. gigas* detected by immunohistochemistry. The cross-sections were stained by Evans blue dye. The green indicates positive signals of *Cg*CLec-3. Negative serum from normal mouse was used as control. The scale bar is 20 μm. (For interpretation of the references to color in this figure legend, the reader is referred to the Web version of this article.)

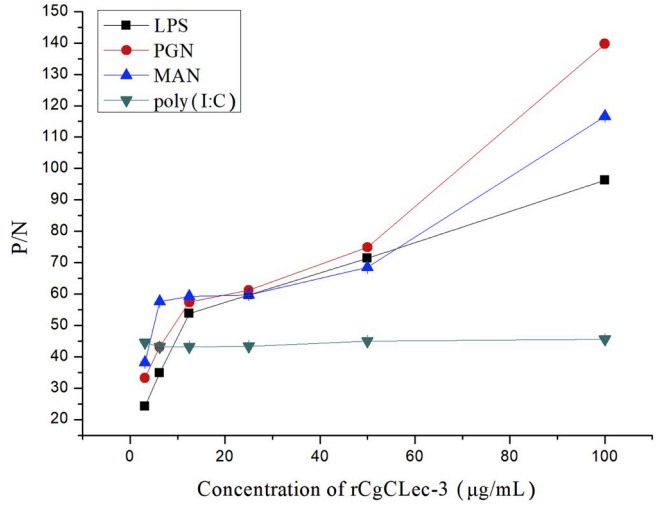

Fig. 6. ELISA analysis of the interaction between r*Cg*CLec-3 and PAMPs. The activities of r*Cg*CLec-3 to LPS, PGN, MAN and poly (I:C) were analyzed by ELISA. Samples with P/N > 2.1 were considered positive. Results are representative of the mean of three replicates ± S.D.

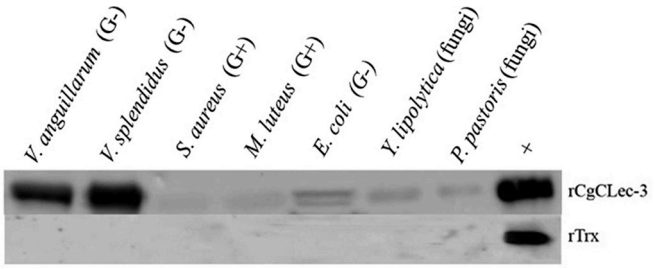

Fig. 7. The microbe binding activity of r*Cg*CLec-3 revealed by Western blot. rTrx was employed as negative, and rTrx's binding activity towards different microbes using anti-His tag antibody.

values of *E. coli* and *S. aureus* were recorded every 30 min for 13 h.

r*Cg*CLec-3 (200 μg/mL) could significantly inhibit the growth of *E. coli* from 3 h to 13 h ($p < 0.05$) compared with the TBS and rTrx groups. While no significant change was observed for the growth of *E. coli* in the r*Cg*CLec-3 (100 μg/mL) group compared with the TBS or rTrx group (Fig. 10A).

The OD_{600} value of *S. aureus* in r*Cg*CLec-3 (200 μg/mL) treatment group was significantly lower ($p < 0.05$) than that in TBS and rTrx groups at 4–16 h post treatment. There was no significant change of OD_{600} value in r*Cg*CLec-3 (100 μg/mL) group, compared to that in TBS and rTrx treatment groups in the whole experimental duration (Fig. 10B).

4. Discussion

CTLs are greatly abundant and diverse in invertebrates, and they play crucial roles by recognizing PAMPs [9], binding or agglutinating pathogen [39], suppressing the growth of pathogen [39], destroying the invading pathogen [40], or enhancing the phagocytosis [27] in the innate immunity. So far, more and more CTLs have been identified in invertebrates. However, the functions and the corresponding molecular binding mechanisms of these diverse CTLs are not well understood. In the present study, a new member of CTLs (*Cg*CLec-3) was identified from Pacific oyster *C. gigas*. Its sequence characteristics and biological activities were investigated to comprehensively understand the roles of CTLs in innate immunity of molluscs.

Accumulating evidences have favored that molluscan CTLs exhibit diversity of CRD structure, which is mainly embodied in the number of CRD as well as the variety of Ca^{2+}-binding site 2 in CRDs. In the present study, *Cg*CLec-3 was identified as a secreted CTL with single CRD, which was similar to the most molluscan CTLs [16,20,21,29,33,41]. The other four CTLs identified in Pacific oyster *C. gigas* all contain a single CRD with different motifs at Ca^{2+}-binding site 2, such as EPN motif in *Cg*CLec-2, QPE in *Cg*CLec-4, and QYE in *Cg*CLec-5. A novel DIN motif was predicted locating at the Ca^{2+}-binding site 2 of *Cg*CLec-3, which had never been found in the previously identified CTLs, indicating the existence of abundant motif in oyster CTLs. As an important PRR, a lot of CTLs from molluscs could be induced by both pathogens and PAMPs [10,24,25]. In the present study, the mRNA expression levels of *Cg*CLec-3 in hemocytes increased significantly after bacterial challenge and PAMP stimulations, indicating its involvement in the immune response against pathogen challenge. The spatial distribution of *Cg*CLec-3 protein was further investigated to explore its possible immune functions. *Cg*CLec-3 protein was mainly detected in both gill and mantle. Gill was reported to be the potential hematopoiesis site of adult oyster [38], and *Cg*CLec-3 was found to be expressed specially on the tubule lumen of gill. Besides, the mantle edge was also reported to be an important area for the development of immunocompetence in the larvae of blue mussel *Mytilus galloprovincialis* [42]. *Cg*CLec-3 protein was strongly expressed on the epidermis, which were the cells directly contacting with environmental microbes. These results collectively indicated that *Cg*CLec-3 could recognize various

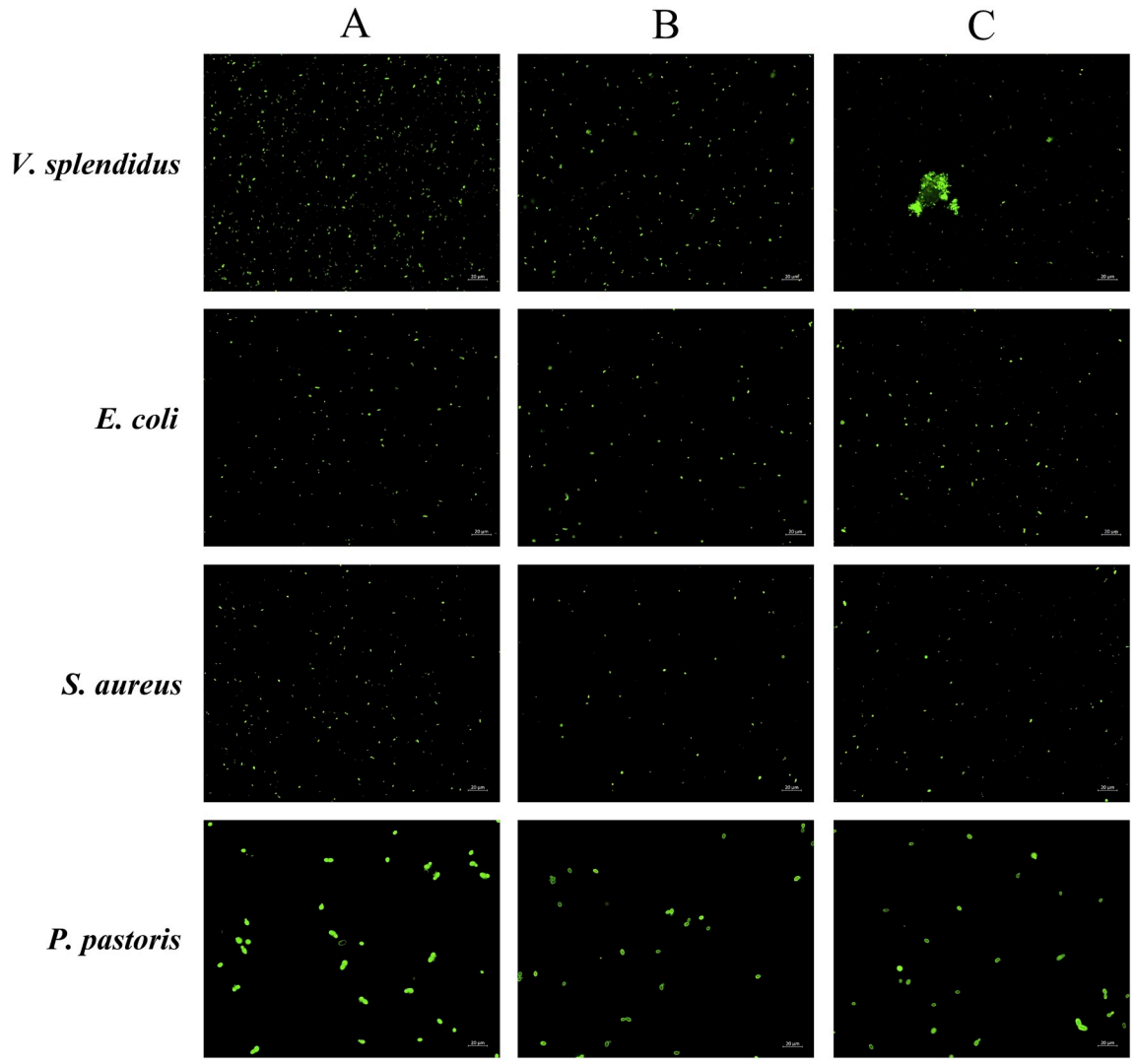

Fig. 8. The microbial agglutinating activity of r*Cg*CLec-3. The FITC-labeled Gram-negative bacteria (*E. coli* and *V. splendidus*), Gram-positive bacteria (*S. aureus*) and fungi (*P. pastoris*) were suspended in TBS (A), rCgCLec-3 without Ca^{2+} (B), and rCgCLec-3 with Ca^{2+} (C).

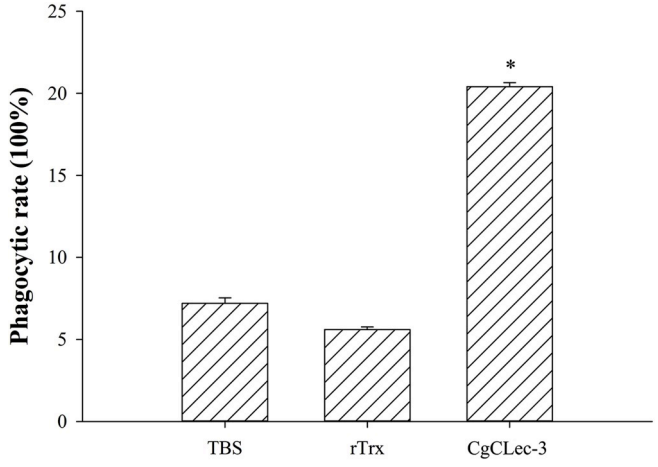

Fig. 9. The enhanced phagocytosis mediated by r*Cg*CLec-3 investigated by flow cytometry. Vertical bars represents the mean ± S.D. (N = 3).

PAMPs as well bacteria, and involved in innate immune response.

The sugar recognition mediated by CTLs benefits from the CRD, which is critical in Ca^{2+}-dependent carbohydrate binding. The CRDs exhibit conservative characteristic in structure, and the conserved motifs at the Ca^{2+}-binding site 2 determine the CRD binding ability [5]. The types of motif vary greatly in molluscs, and many kinds of novel motifs have been identified in molluscan CTLs. In the present study, *Cg*CLec-3 contained a novel DIN motif, which had never been reported in invertebrate CTLs. *Cg*CLec-3 displayed strong binding affinity to PGN, moderate affinity to MAN and LPS, but no affinity to poly (I:C). Similar to most identified molluscan CTLs with novel motifs, *Cg*CLec-3 exhibited a broader recognition spectrum. The PAMP recognition and binding spectrum of *Cg*CLec-3 is consistent with that of *Cf*Lec-1 from *C. farreri* [27], which contains an EPD motif. Previous studies found that some molluscan CTLs with different motif at the Ca^{2+}-binding site 2 displayed similar PAMP and microbial binding spectrums, which is significant different from the specific recognition mechanism in vertebrate. It was suspected that the diversity of motif at the Ca^{2+}-binding site 2 endowed the CTLs with the capacity to recognize and bind various microorganisms and PAMPs in invertebrates. CTLs specifically bind PAMPs on the surfaces of many pathogens, which provide them with the capacity to recognize a wide variety of pathogens. In the present study, *Cg*CLec-3 could recognize and bind yeasts *Y. lipolytica* and *P. pastoris*, and Gram negative bacteria *V. splendidus*, *V. auguillarum* and *E. coli*, and displayed very weak binding affinity to Gram positive bacteria *S. aureus and M. luteus*. The results of microbe binding spectrum further

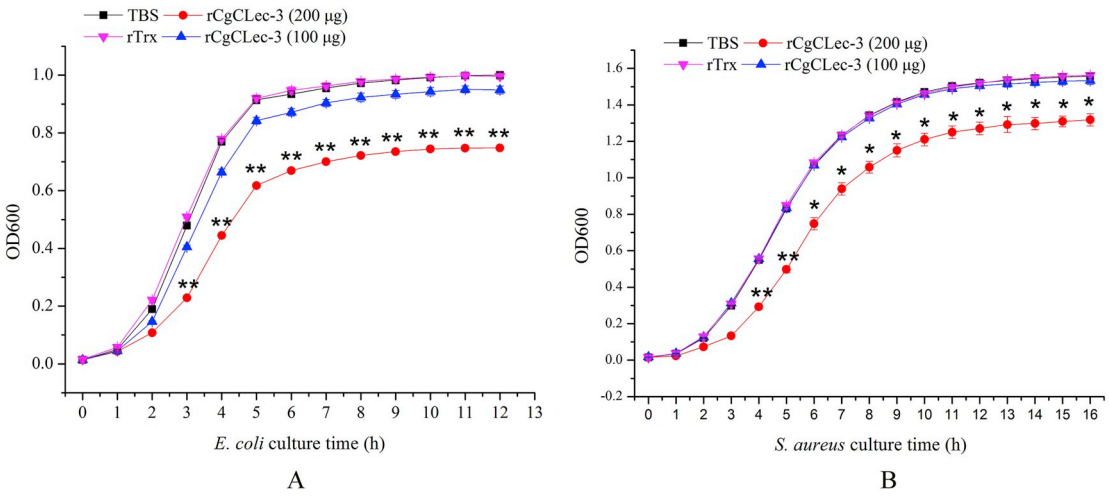

Fig. 10. Antimicrobial activity assay detected by growth curve of *E. coli* (A) and *S. aureus* (B). TBS and rTrx were used as blank and negative control, respectively.

supported the broad PAMP binding spectrum of *Cg*CLec-3. It was worth noting that *Cg*CLec-3 exhibited very strong binding activity towards PGN *in vitro*, and the expression level of *Cg*CLec-3 mRNA was dramatically up-regulated after PGN stimulation. However, r*Cg*CLec-3 showed weak binding affinity to Gram positive bacteria *S. aureus and M. luteus*. These phenomena tempted us to suspect that the involvement of *Cg*CLec-3 in Gram positive bacteria recognition might need the assistance of other molecule. Further research is still needed to better understand the underlying mechanism. The most important feature of CTLs is to bind specific carbohydrates on the cell surface and agglutinate cells in the presence of Ca^{2+} [5]. The previous studies, some single CRD CTLs were reported to agglutinate limited microbes, such as *Cf*Lec-2 from *C. farreri* could only agglutinate *S. haemolyticus* [28]. In the present study, *Cg*CLec-3 could only agglutinate *V. splendidus* in a Ca^{2+}-dependent manner. These results collectively indicated that *Cg*CLec-3 might act as carbohydrate-sensing proteins in the innate immunity of oyster, with binding capability to broad spectrum of PAMPs and microbes, as well as agglutinating property towards *V. splendidus*.

Opsonins are host-derived proteins that could enhance the phagocytic ability and diversify the functional repertoire of phagocytes [43]. Phagocytosis is initiated by the binding of bacteria to phagocytes, and the process is facilitated by C3bi or specific Igs in vertebrate [44]. There are increasing evidences that some PRRs, such as CTLs and PGRP-LC, could enhance the activity of phagocytes toward senescent (i.e., apoptotic) cells or bacteria [45,46]. Molluscan CTLs have been reported to play significant roles in hemocyte phagocytosis and encapsulation. For instance, *Cg*CLec-2 from *C. gigas* [16], *Cf*Lec-1 and *Cf*Lec-4 from *C. farreri* [27,47], and *Ai*CTL-3 from *A. irradians* [17] could work in a similar manner as vertebrate Igs or C3bi to mediate and enhance phagocytosis. In the present study, *Cg*CLec-3 could recognize and bind the bacteria component, as well as bind to the surface of hemocytes, and the multi-directed binding was suspected to be responsible for the phagocytosis mediated by *Cg*CLec-3. Previous reports have revealed that some PRRs could function as effector molecules involved in a direct attack on infectious agents [41]. In molluscs, several CTLs exhibited growth suppression activity against microbes, such as *Cg*CLec-2 and *Cg*CLec-4 from Pacific oyster *C. gigas* [16,41], MCL from Manila clam *R. philippinarum* [23, 48], AiCTL-7 from *A. irradians* [20], *Cf*Lec-1 and *Cf*Lec-2 from *C. farreri* [27,28]. In the present study, r*Cg*CLec-3 exhibited antibacterial effects on Gram-negative bacteria *E. coli* and Gram-positive bacteria *S. aureus*. The immobilization of bacteria, binding and destruction of bacteria cell walls were believed to be the main mechanisms to inhibit and terminate the microorganism growth [31]. Although the exact mechanism of growth suppression activity of *Cg*CLec-3 remains unknown, the cell membrane destruction led by the binding and interaction of *Cg*CLec-3 with bacteria was hypothesized to be the main mechanism [40]. All these studies indicated that *Cg*CLec-3 could also contribute to the host defense mechanisms as an effector molecule.

Five CTLs have been so far identified from Pacific oyster *C. gigas*, and all of them contain a single CRD with different motif at the Ca^{2+}-binding site 2. Except for *Cg*CLec-1 (only expressed in the digestive gland) [33], other four CTLs all can be induced by *V. splendidus* or PAMP stimulations [16,41], indicating their involvement in the immune responses against the invaders. These four CTLs exhibited similar PAMP and microbe binding spectrum, but showed agglutination and antimicrobial activity towards different bacteria. For instance, *Cg*CLec-3 only agglutinated Gram-negative bacteria *V. splendidus*, while *Cg*CLec-4 agglutinated Gram-positive bacteria *S. aureus*, Gram-negative bacteria *E. coli* and *V. anguillarum*, as well as fungi *Y. lipolytica* [41]. *Cg*CLec-2, *Cg*CLec-3 and *Cg*CLec-4 exhibited antibacterial activity towards different bacteria [16,41], while *Cg*CLec-5 had no obvious antibacterial activity [41]. All the results collectively indicate that CTLs in oyster are a superfamily of diverse proteins with specificity in recognition, and complementarity in function, which would provide a prominent immune defense network for oyster against invaders.

In conclusion, a C-type lectin with a novel DIN motif was identified from the Pacific oyster *C. gigas*. The mRNA expression of *Cg*CLec-3 could be induced by PAMP and bacterial stimulations. *Cg*CLec-3 could recognize a variety of PAMPs and agglutinate microorganisms, and also enhance the phagocytic ability of hemocytes to *V. splendidus* and inhibit the growth of *E. coli* and *S. aureus*. Given the versatile functions of *Cg*CLec-3, it was suspected that *Cg*CLec-3 involved in innate immunity of oysters via recognizing and binding to specific PAMPs of invading pathogen, and triggering phagocytosis as well as antibacterial activity, as a coordination factor of both cellular and humoral immune response.

Acknowledgements

We are grateful to all the laboratory members for their technique advice and helpful discussions. This research was supported by a grant from National key R&D Program of China (2018YFD0900502), a grant from National Science Foundation of China (U1706204), Distinguished Professor of Liaoning, Dalian High Level Talent Innovation Support Program (2015R020), the Research Foundation for Aoshan Talent Cultivation Program Supported by Qingdao National Laboratory for Marine Science, Earmarked Fund (CARS-49) from Modern Agro-industry Technology Research System, and Technology and Talented Scholars in Dalian Ocean University, and Natural Science Foundation of Liaoning, China (20170520056).

Appendix A. Supplementary data

Supplementary data to this article can be found online at https://doi.org/10.1016/j.fsi.2019.07.001.

References

[1] P.C. Hanington, M.A. Forys, J.W. Dragoo, S.M. Zhang, C.M. Adema, E.S. Loker, Role for a somatically diversified lectin in resistance of an invertebrate to parasite infection, Proc. Natl. Acad. Sci. U. S. A. 107 (2010) 21087–21092.

[2] T. Fujita, M. Matsushita, Y. Endo, The lectin-complement pathway–its role in innate immunity and evolution, Immunol. Rev. 198 (2004) 185–202.

[3] H. Chu, S.K. Mazmanian, Innate immune recognition of the microbiota promotes host-microbial symbiosis, Nat. Immunol. 14 (2013) 668–675.

[4] C.A. Janeway Jr., R. Medzhitov, Innate immune recognition, Annu. Rev. Immunol. 20 (2002) 197–216.

[5] A. Cambi, M. Koopman, C.G. Figdor, How C-type lectins detect pathogens, Cell Microbiol. 7 (2005) 481–488.

[6] I.M. Dambuza, G.D. Brown, C-type lectins in immunity: recent developments, Curr. Opin. Immunol. 32 (2015) 21–27.

[7] W.I. Weis, M.E. Taylor, K. Drickamer, The C-type lectin superfamily in the immune system, Immunol. Rev. 163 (1998) 19–34.

[8] N. Wang, I. Whang, J. Lee, A novel C-type lectin from abalone, *Haliotis discus discus*, agglutinates Vibrio alginolyticus, Dev. Comp. Immunol. 32 (2008) 1034–1040.

[9] J. Yang, M. Huang, H. Zhang, L. Wang, H. Wang, L. Wang, et al., CfLec-3 from scallop: an entrance to non-self recognition mechanism of invertebrate C-type lectin, Sci. Rep. 5 (2015) 10068.

[10] L. Wang LW, M. Huang, H. Zhang, The immune role of C-type lectins in molluscs, ISJ-Invert Surviv. J. (2011) 241–246.

[11] G. Zhang, X. Fang, X. Guo, L. Li, R. Luo, F. Xu, et al., The oyster genome reveals stress adaptation and complexity of shell formation, Nature 490 (2012) 49–54.

[12] H. Zhang, H. Wang, L. Wang, X. Song, J. Zhao, L. Qiu, et al., A novel C-type lectin (Cflec-3) from *Chlamys farreri* with three carbohydrate-recognition domains, Fish Shellfish Immunol. 26 (2009) 707–715.

[13] H. Zhang, H. Wang, L. Wang, L. Song, X. Song, J. Zhao, et al., Cflec-4, a multi-domain C-type lectin involved in immune defense of Zhikong scallop *Chlamys farreri*, Dev. Comp. Immunol. 33 (2009) 780–788.

[14] L. Wang, L. Wang, J. Yang, H. Zhang, M. Huang, P. Kong, et al., A multi-CRD C-type lectin with broad recognition spectrum and cellular adhesion from *Argopecten irradians*, Dev. Comp. Immunol. 36 (2012) 591–601.

[15] T. Talaei-Khozani, M. Monsefi, M. Ghasemi, Lectins influence chondrogenesis and osteogenesis in limb bud mesenchymal cells, Glycoconj. J. 28 (2011) 89–98.

[16] H. Li, H. Zhang, S. Jiang, W. Wang, L. Xin, H. Wang, et al., A single-CRD C-type lectin from oyster *Crassostrea gigas* mediates immune recognition and pathogen elimination with a potential role in the activation of complement system, Fish Shellfish Immunol. 44 (2015) 566–575.

[17] M. Huang, X. Song, J. Zhao, C. Mu, L. Wang, H. Zhang, et al., A C-type lectin (AiCTL-3) from bay scallop *Argopecten irradians* with mannose/galactose binding ability to bind various bacteria, Gene 531 (2013) 31–38.

[18] M. Huang, L. Wang, J. Yang, H. Zhang, L. Wang, L. Song, A four-CRD C-type lectin from *Chlamys farreri* mediating nonself-recognition with broader spectrum and opsonization, Dev. Comp. Immunol. 39 (2013) 363–369.

[19] L.L. Zhao, Y.Q. Wang, Y.J. Dai, L.J. Zhao, Q. Qin, L. Lin, et al., A novel C-type lectin with four CRDs is involved in the regulation of antimicrobial peptide gene expression in *Hyriopsis cumingii*, Fish Shellfish Immunol. 55 (2016) 339–347.

[20] P. Kong, L. Wang, H. Zhang, X. Song, Z. Zhou, J. Yang, et al., A novel C-type lectin from bay scallop *Argopecten irradians* (AiCTL-7) agglutinating fungi with mannose specificity, Fish Shellfish Immunol. 30 (2011) 836–844.

[21] H. Zhang, X. Song, L. Wang, P. Kong, J. Yang, L. Liu, et al., AiCTL-6, a novel C-type lectin from bay scallop *Argopecten irradians* with a long C-type lectin-like domain, Fish Shellfish Immunol. 30 (2011) 17–26.

[22] X. Jing, E.P. Espinosa, M. Perrigault, B. Allam, Identification, molecular characterization and expression analysis of a mucosal C-type lectin in the eastern oyster, *Crassostrea virginica*, Fish Shellfish Immunol. 30 (2011) 851–858.

[23] K.G. Takahashi, T. Kuroda, K. Muroga, Purification and antibacterial characterization of a novel isoform of the Manila clam lectin (MCL-4) from the plasma of the Manila clam, *Ruditapes philippinarum*, Comp. Biochem. Physiol. B Biochem. Mol. Biol. 150 (2008) 45–52.

[24] L. Wang, X. Song, L. Song, The oyster immunity, Dev. Comp. Immunol. 80 (2018) 99–118.

[25] W. Wang, X. Song, L. Wang, L. Song, Pathogen-derived carbohydrate recognition in molluscs immune defense, Int. J. Mol. Sci. 19 (2018) 3.

[26] Y.S. Kang, Y.M. Kim, K.I. Park, S. Kim Cho, K.S. Choi, M. Cho, Analysis of EST and lectin expressions in hemocytes of Manila clams (*Ruditapes philippinarum*) (Bivalvia: Mollusca) infected with Perkinsus olseni, Dev. Comp. Immunol. 30 (2006) 1119–1131.

[27] J. Yang, L. Wang, H. Zhang, L. Qiu, H. Wang, L. Song, C-type lectin in *Chlamys farreri* (CfLec-1) mediating immune recognition and opsonization, PLoS One 6 (2011) e17089.

[28] J. Yang, L. Qiu, X. Wei, L. Wang, L. Wang, Z. Zhou, et al., An ancient C-type lectin in *Chlamys farreri* (CfLec-2) that mediate pathogen recognition and cellular adhesion, Dev. Comp. Immunol. 34 (2010) 1274–1282.

[29] C. Mu, X. Song, J. Zhao, L. Wang, L. Qiu, H. Zhang, et al., A scallop C-type lectin from *Argopecten irradians* (AiCTL5) with activities of lipopolysaccharide binding and Gram-negative bacteria agglutination, Fish Shellfish Immunol. 32 (2012) 716–723.

[30] M.J. Demaintenon, Phylogeny and evolution of the Mollusca, Bull. Marine Sci. Miami 83 (2008) 435–437.

[31] X.K. Jin, S. Li, X.N. Guo, L. Cheng, M.H. Wu, S.J. Tan, et al., Two antibacterial C-type lectins from crustacean, *Eriocheir sinensis*, stimulated cellular encapsulation in vitro, Dev. Comp. Immunol. 41 (2013) 544–552.

[32] L. Zhang, L. Li, X. Guo, G.W. Litman, L.J. Dishaw, G. Zhang, Massive expansion and functional divergence of innate immune genes in a protostome, Sci. Rep. 5 (2015) 8693.

[33] K. Yamaura, K.G. Takahashi, T. Suzuki, Identification and tissue expression analysis of C-type lectin and galectin in the Pacific oyster, *Crassostrea gigas*, Comp. Biochem. Physiol. B Biochem. Mol. Biol. 149 (2008) 168–175.

[34] M. Huang, H. Zhang, S. Jiang, L. Wang, R. Liu, Q. Yi, et al., An EPD/WSD motifs containing C-type lectin from *Argopectens irradians* recognizes and binds microbes with broad spectrum, Fish Shellfish Immunol. 43 (2015) 287–293.

[35] K.J. Livak, T.D. Schmittgen, Analysis of relative gene expression data using real-time quantitative PCR and the 2(-Delta Delta C(T)) Method, Methods 25 (2001) 402–408.

[36] P.K. Smith, R.I. Krohn, G.T. Hermanson, A.K. Mallia, F.H. Gartner, M.D. Provenzano, et al., Measurement of protein using bicinchoninic acid, Anal. Biochem. 150 (1985) 76–85.

[37] S. Cheng, W. Zhan, J. Xing, X. Sheng, Development and characterization of monoclonal antibody to the lymphocystis disease virus of Japanese flounder *Paralichthys olivaceus* isolated from China, J. Virol. Methods 135 (2006) 173–180.

[38] M. Jemaa, N. Morin, P. Cavelier, J. Cau, J.M. Strub, C. Delsert, Adult somatic progenitor cells and hematopoiesis in oysters, J. Exp. Biol. 217 (2014) 3067–3077.

[39] X. Huang, Y. Huang, Y.R. Shi, Q. Ren, W. Wang, Function of a novel C-type lectin with two CRD domains from *Macrobrachium rosenbergii* in innate immunity, Dev. Comp. Immunol. 49 (2015) 121–126.

[40] Y. Yu, Y. Yu, H. Huang, K. Feng, M. Pan, S. Yuan, et al., A short-form C-type lectin from amphioxus acts as a direct microbial killing protein via interaction with peptidoglycan and glucan, J. Immunol. 179 (2007) 8425–8434.

[41] Z. Jia, H. Zhang, S. Jiang, M. Wang, L. Wang, L. Song, Comparative study of two single CRD C-type lectins, CgCLec-4 and CgCLec-5, from pacific oyster *Crassostrea gigas*, Fish Shellfish Immunol. 59 (2016) 220–232.

[42] P. Balseiro, R. Moreira, R. Chamorro, A. Figueras, B. Novoa, Immune responses during the larval stages of *Mytilus galloprovincialis*: metamorphosis alters immunocompetence, body shape and behavior, Fish Shellfish Immunol. 35 (2013) 438–447.

[43] L.M. Stuart, R.A. Ezekowitz, Phagocytosis: elegant complexity, Immunity 22 (2005) 539–550.

[44] O.V. Vieira, R.J. Botelho, S. Grinstein, Phagosome maturation: aging gracefully, Biochem. J. 366 (2002) 689–704.

[45] M. Ramet, P. Manfruelli, A. Pearson, B. Mathey-Prevot, R.A. Ezekowitz, Functional genomic analysis of phagocytosis and identification of a Drosophila receptor for E. coli, Nature 416 (2002) 644–648.

[46] E. Ling, X.Q. Yu, Cellular encapsulation and melanization are enhanced by immulectins, pattern recognition receptors from the tobacco hornworm *Manduca sexta*, Dev. Comp. Immunol. 30 (2006) 289–299.

[47] M. Huang, L. Wang, H. Zhang, C. Yang, R. Liu, J. Xu, et al., The sequence variation and functional differentiation of CRDs in a scallop multiple CRDs containing lectin, Dev. Comp. Immunol. 67 (2017) 333–339.